ACS APPLIED MATERIALS & INTERFACES

Research Article

www.acsami.org

Graphene Oxide Sheets Immobilized Polystyrene for Column Preconcentration and Sensitive Determination of Lead by Flame Atomic Absorption Spectrometry

Aminul Islam,* Hilal Ahmad, Noushi Zaidi, and Suneel Kumar

Analytical Research Laboratory, Department of Chemistry, Aligarh Muslim University, Aligarh, India 202 002

Supporting Information

ABSTRACT: A novel solid-phase extractant was synthesized by coupling graphene oxide (GO) on chloromethylated polystyrene through an ethylenediamine spacer unit to develop a column method for the preconcentration/separation of lead prior to its determination by flame atomic absorption spectrometry. It was characterized by Fourier transform infrared spectroscopy, far-infrared spectroscopy, thermogravimetric analysis/differential thermal analysis, scanning electron microscopy, energy-dispersive spectrometry, and transmission electron microscopy. The abundant oxygen-containing surface functional groups form a strong complex with lead, resulting in higher sorption capacity (227.92 mg g^{-1}) than other nanosorbents used for sorption studies of the column method. Using the column procedure here is an alternative to the direct use of GO, which restricts irreversible aggregation of GO and its escape into the ecosystem, making it an environmentally sustainable method. The column method was optimized by varying experimental variables such as pH, flow rate for sorption/desorption, and elution condition and was observed to exhibit a high preconcentration factor (400) with a low preconcentration limit (2.5 ppb) and a high degree of tolerance for matrix ions. The accuracy of the proposed method was verified by determining the Pb content in the standard reference materials and by recovery experiments. The method showed good precision with a relative standard deviation <5%. The proposed method was successfully applied for the determination of lead in tap water, electroplating wastewater, river water, and food samples after preconcentration.

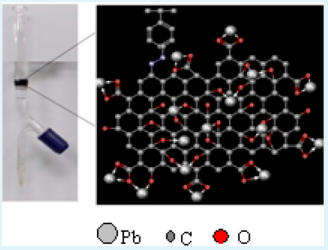

KEYWORDS: *graphene oxide, lead, column preconcentration, atomic absorption spectrometry*

INTRODUCTION

With growing industrialization and urbanization, diversified uses of metals in varied forms have become a significant source of pollution resulting in environmental deterioration. The indication of their importance relative to other potential hazards is their ranking by the U.S. Agency for Toxic Substances and Disease Registry, which lists lead (Pb) as first among all hazards present in the toxic waste sites according to their prevalence and the severity of their toxicity.[1] Pb is also among the 14 priority PBTs (persistent, bioaccumulative, and toxic) listed by the U.S. Environmental Protection Agency (USEPA) in 1999. It poses a serious threat to public health due to its ubiquitous environmental presence and because it is a neurotoxicant and causes suppression of hemoglobin biosynthesis.[2−4] Pb exposure occurs through contaminated air, food, and water. The USEPA has set the action level for Pb in water at 15 $\mu g\ L^{-1}$.[5] The World Health Organization has set a maximum permissible limit of 10 $\mu g\ L^{-1}$ for lead in drinking water.[6] Quantification of Pb is the foremost step to check the level of contamination, monitor the efficiency of the action plan taken to control the pollution, and assess the effects of exposure on biota. Hence, development of sensitive, accurate, selective, and economical methods for the trace determination of Pb in environmental and biological samples is of paramount importance in environmental analytical chemistry. Recently, the sensitive determination of lead involving quantum dots,[7] gold nanoparticles,[8] DNAzymes and aptamers,[9] and DNAzyme modified gold nanoparticles and graphene oxide[10] have been reported. However, due to low concentrations of metal ions and matrix interferences, the determination of metal ions in complex matrices requires preconcentration and/or separation of analytes to improve accuracy, sensitivity, and selectivity.[11−13]

In past decades, solid-phase extraction (SPE) has played a crucial role in the field of separation science not only to isolate analyte of interest from a great variety of sample matrices,[14,15] but also to concentrate the analytes prior to their determination by low-cost and less sensitive techniques.[16−20] Currently, use of nanomaterials such as sulfur nanoparticles,[21] yeast immobilized TiO_2,[22] carbon nanotubes (CNTs),[23,24] fullerenes,[25] carbon nanohorn,[26] activated carbon,[27,28] and carbon nanocones/disks[29] in SPE has become an active area of research in the field of separation science due to their unique properties, such as large surface area and high mechanical strength.[13,21−31] Among them, CNTs possess great potential to remove metal ions and organic pollutants from aqueous solutions and have therefore been used as a superior adsorbent for wastewater treatment.

Received: May 20, 2014
Accepted: July 8, 2014
Published: July 8, 2014

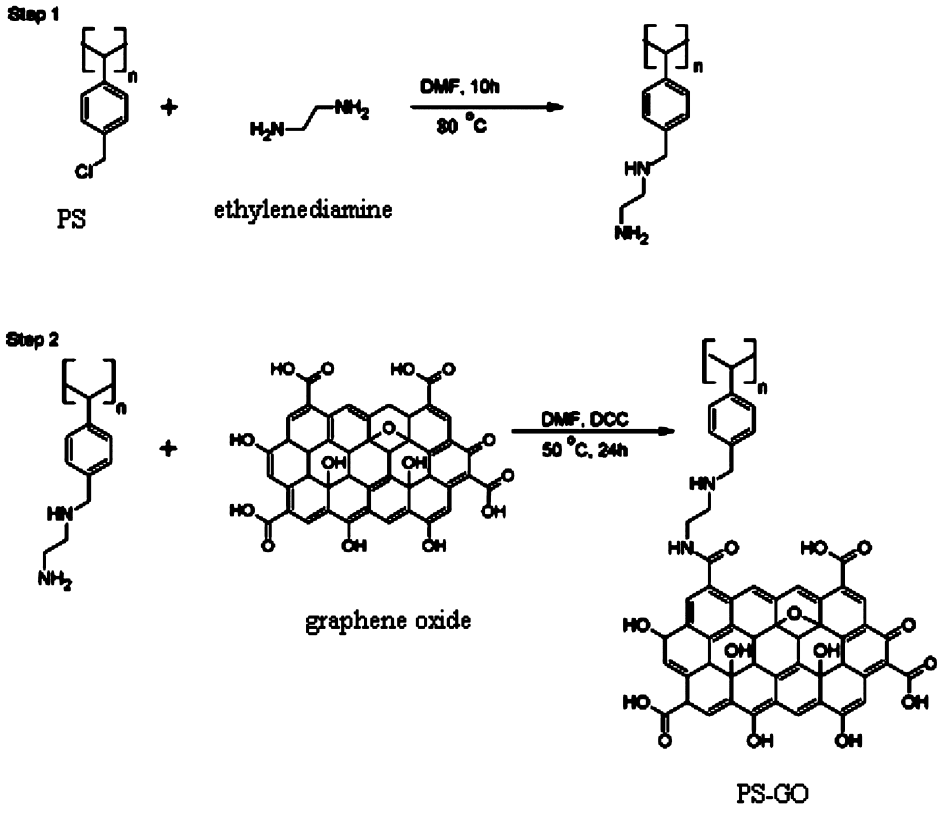

Figure 1. Immobilization of GO on polymeric resin beads.

However, CNTs usually contain large amounts of residual metallic impurities from the metal catalysts used in their synthesis. These impurities may have a negative influence on the applications of CNTs,[23,30,31] and large-scale applications of CNTs are limited because of comparatively higher operational cost.

Graphene and graphene oxide (GO), a two-dimensional (2D) honeycomb carbon lattice with high specific surface area and remarkable mechanical, structural, electrical, and thermal properties,[32−36] show relentless perspectives in nanoelectronics,[37] sensors,[38] supercapacitors,[39] composite materials,[39,40] and environmental applications[41−48] and are considered more propitious than other carbonaceous nanomaterials. Pure GO with numerous epoxy (−COC), hydroxyl (−OH), carbonyl (−CO), and carboxyl (−COOH) groups[42,49] can be synthesized by oxidizing graphite in a single step without the use of a metal catalyst. The introduction of abundant oxygen containing functional groups at GO surface leads to the development of highly hydrophilic character and active sites for metal ion complexation, making it a potential SPE sorbent and substitute for CNTs.

In recent reports, the adsorption properties of GO for metal ions have been studied, and their sorption capacities (mg g^{-1}) were reported as 46.6 (Cu),[41] 106.3 (Cd),[42] 68.2 (Co),[42] and 842, 1119 (Pb).[43,44] The following published data indicates that GO can be an ideal matrix for the removal/preconcentration of metal ions from environmental samples: arsenic,[45] lanthanides and actinides,[46] Cu and fulvic acid,[47] Pb, Cd, Bi, and Sb.[48] These studies dealt with the adsorption of metal ions on dispersed GO only by batch method using either 0.22 μm membrane filters, centrifugation, addition of sodium chloride, or magnetic separation to separate the GO from the sample solution. However, such a separation method restricts the use of large sample volumes and essentially requires a column operation. Direct and multiple use of GO in wastewater treatment separation and recycling of GO becomes challenging, particularly when the sheet size goes down to nanoscale. Owing to the strong van der Waals and $\pi-\pi$ stacking interactions, GO tends to aggregate in batch method, which can significantly affect the efficiency and reusability of GO as it requires sonication to redisperse before its use in the next sorption cycle. In flow-through column SPE, miniscule GO may escape from the cartridge due to the polydispersity of GO sheets.[50] These released GO sheets are detrimental and pose a potential health threat to ecosystems.[51,52] To simultaneously combat these analytical challenges and prevent environmental consequences, we suggest for the first time the use of polymer-bound GO sheets as a solid-phase extractant in a continuous flow system.

In this work, we report a novel solid-phase matrix fabricated by the covalent coupling of GO with polystyrene beads through ethylenediamine spacer unit for preconcentration/separation of Pb^{2+} from large environmental sample volumes by column operation. The chemical reaction engineered to couple the GO on polystyrene beads provides high structural stability with the spacer unit, which enables GO to attain its 2D conformations and makes accessible both sides of the GO surface to retain analyte ion, thus enhancing better analyte recognition. Such an organized topological configuration also contributes to high mechanical strength. The polymer-bound GO sheets restrict the irreversible aggregation of GO and leaching from the column, as compared to direct use of GO facilitating the reduction of operation time for each complete sorption/elution cycle.

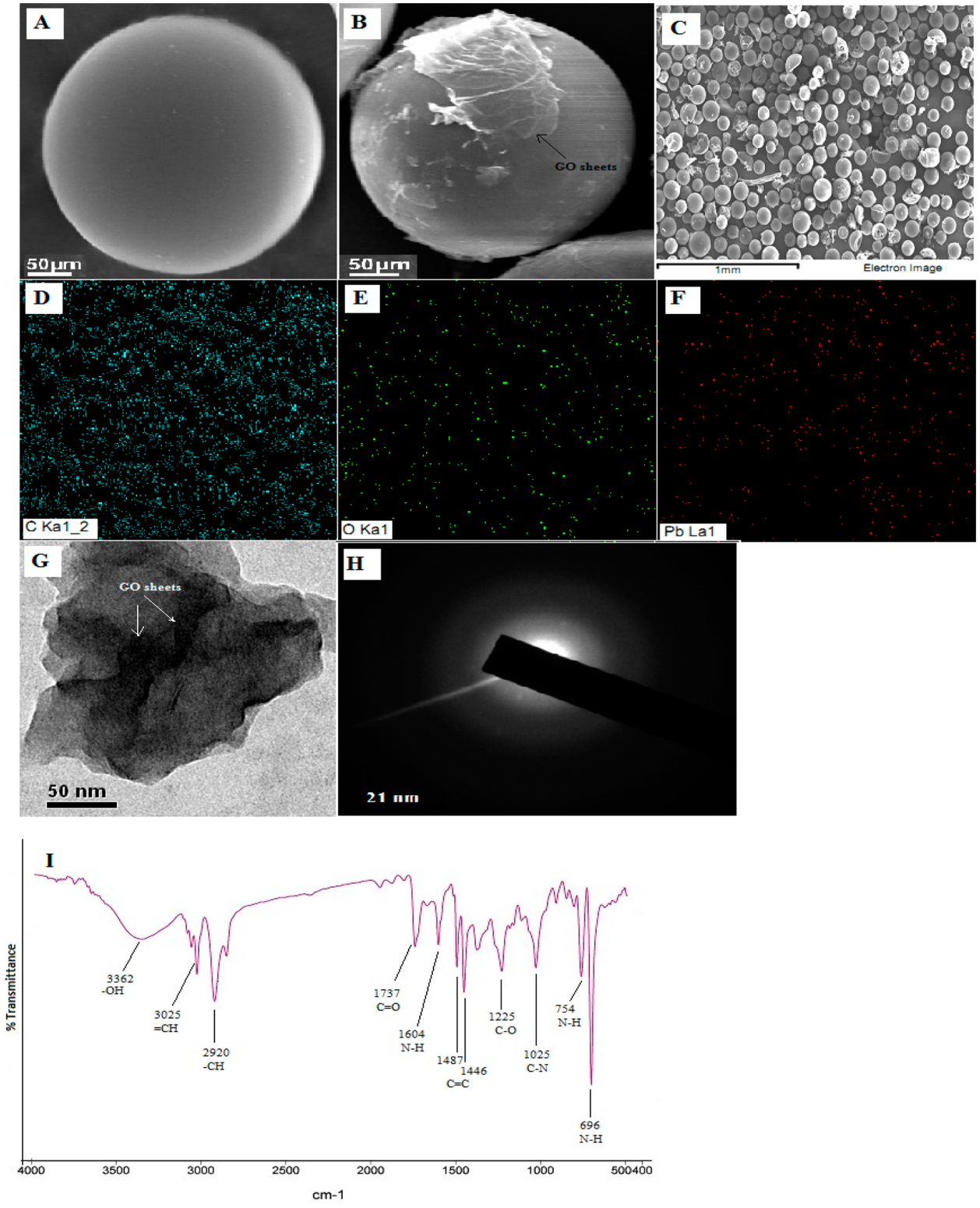

Figure 2. SEM images of (A) bare PS resin bead, (B) single PS-GO resin bead, and (C) cluster of PS-GO resin beads. (D–F) the corresponding elemental mapping images of C, O, and Pb, respectively. (G) TEM image of PS-GO. (H) SAED pattern image of PS-GO. (I) FT-IR spectra of PS-GO.

MATERIALS AND METHODS

Reagents and Solutions. All chemicals used were of analytical reagent grade. Stock solution of lead nitrate (1000 mg L^{-1}) was purchased from Merck (Mumbai, India). The chloromethylated polystyrene resin (PS) and graphite powder (50 μm) were procured from Sigma-Aldrich (Steinem, Germany) and Otto Chemie Pvt. Ltd. (Mumbai, India), respectively. Environmental standard reference material (SRM), vehicle exhaust particulates (NIES 8), and biological SRM (citrus leaves, SRM 1572) were obtained from the National Institute of Environmental Studies (Ibaraki, Japan) and the National Bureau of Standards, U.S. Department of Commerce (Washington, DC).

Preparation of Graphene Oxide. GO was prepared from natural graphite powders by a modified Hummers method.[53] The prepared carboxy rich GO sheets were immobilized on resin in the subsequent step.

Immobilization of GO on Polymeric Resin. In this procedure, first, the amine terminated polystyrene resin was prepared by reacting PS with ethylenediamine. The 5.0 g of PS was swelled in 30 mL of dimethylformamide (DMF) for 2 h and refluxed with a solution of ethylenediamine (2.5 g in 20 mL of DMF) for 10 h. After the mixture cooled, the amine terminated resin was filtered and washed thoroughly with DMF and TDW. GO was immobilized onto the amine functionalized host polymeric resin by coupling an amine group and a carboxylic functionality of the resin beads and the GO, respectively, using *N,N′*-dicyclohexylcarbodiimide (DCC) as a coupling agent.[54] To link GO onto the modified resin, 10 mL of GO solution (2 mg mL^{-1}) was placed into a 250 mL round-bottom flask in a 40 mL DMF, and then 1 g of DCC and amine terminated polystyrene resin were added. The reaction mixture was stirred for 24 h at 50 °C. After the reaction mixture cooled, it was filtered under suction and washed sequentially with DMF and TDW to remove uncoupled GO, and it was dried at 50 °C for 12 h. The synthesis scheme is shown in Figure 1, and the product was abbreviated as PS-GO.

Characterization of PS-GO. The synthesized PS-GO resin was characterized by Fourier transform infrared spectra (FT-IR) from a PerkinElmer Spectrum Two spectrometer (Waltham, MA) using KBr disk method in the range of 500−4000 cm^{-1} with a resolution of 2.0 cm^{-1}, and the interferograms were recorded by accumulating 32 scans. Far-infrared spectra (FIR) measurements were obtained by using a PerkinElmer spectrometer in polyethylene pellet under nitrogen atmosphere at room temperature (27 °C) in the range of 50−500 cm^{-1}. To characterize the amide bond in PS-GO a solid state, ^{13}C cross polarization−magic angle spinning (CP/MAS) NMR spectra were recorded using a Jeol JNM-ECA400 spectrometer (Peabody, MA) operating at 400 MHz. Surface area analysis measurements were done on an Autosorb-iQ one-station gas sorption analyzer (Quantachrome Instruments, Boynton Beach, FL). A Shimadzu TGA/DTA simultaneous measuring instrument, DTG-60/60H (Kyoto, Japan) was used for thermogravimetric analysis (TGA) and differential thermal analysis (DTA) at temperatures of 50−600 °C at a heating rate of 10 °C min^{-1} and under an inert atmosphere (N_2 flow rate of 50 mL min^{-1}). Scanning electron microscopy (SEM) images for microstructural observations and energy dispersive X-ray analysis (EDS) spectra for micro compositional analysis of the resin were examined with a Jeol JSM-6510LV (Tokyo, Japan) after-coated with a gold overlayer to avoid charging during electron irradiation. Transmission electron microscope (TEM) images were obtained using a Jeol JEM-2100 microscope (Peabody, MA).

Pretreatment of Samples and SRMs. The river water (the Ganga, Narora, India), electroplating industry wastewater (Aligarh, India), and tap water (Laboratory, Department of Chemistry) were filtered through a cellulose membrane filter (Millipore) of 0.45 μm pore size, acidified to pH 2 with concentrated HNO_3, and stored in precleaned polyethylene bottles, while the food samples (rice and grams) were purchased from a local market (Aligarh, India) and digested (1 g of each) by wet oxidation with concentrated HNO_3, $HClO_4$, and 30% H_2O_2.[17] The residue was dissolved in 2 mL of 0.5 M HNO_3 and finally made up to 100 mL with triply distilled water (TDW). The solution of NIES 8 was prepared as reported in earlier work,[55,56] and SRM 1572 was prepared by dissolving 0.376 g of dried SRM sample (dried for 2 h in an oven at 85 °C) in 10 mL of concd HNO_3. After adding 0.5 mL of 30% H_2O_2, we evaporated the solution near dryness. The obtained residue was dissolved in 2 mL of 0.5 M HNO_3 and made up to a 100 mL volume in a calibrated flask.

Optimized Method for Sorption and Desorption Studies of Pb^{2+}. To optimize sorption/desorption of Pb^{2+} using solid-phase extraction, the univariate approach was followed to establish all the experimental parameters. Each optimum condition was established by varying one of them and following the recommended procedure. A batch method was preferred to study the effect of pH, stirring time, and sorption isotherms. The other experimental variables were optimized using column method. Concentration of Pb^{2+} was determined using a GBC 932+ flame atomic absorption spectrometer (FAAS, Dandenong, Australia) with deuterium background correction at 217.0 nm (slit width, 0.5 nm) on an air-acetylene flame.

Batch Equilibrium Sorption Procedure. PS-GO (100 mg) was stirred with 50 mL of Pb^{2+} (750 mg L^{-1}), and the solution was maintained at constant pH using suitable buffer solutions at 27 ± 0.2 °C for 50 min. The PS-GO was filtered using a 0.45 μm pore size cellulose membrane filter (Millipore). The concentration of Pb^{2+} in the filtrate was measured by FAAS.

Fixed-Bed Column Procedure. All column experiments were carried out in a glass column (10 cm × 1.0 cm) fitted with a porous disc (J-SIL Scientific Industries, Agra, India). The column was slurry packed with water-soaked PS-GO (200 mg) with a bed height of 1.0 cm and preconditioned with 5 mL of buffer solution with a pH of 7.5. The 100 mL of Pb^{2+} solution (50 μg L^{-1}) buffered to pH 7.5 ± 0.1 was passed through the column at a flow rate of 5 mL min^{-1}. The column was then washed with TDW to ensure complete removal of unretained Pb^{2+} and that sorbed Pb^{2+} was desorbed by passing 5 mL of 2 M HCl at a flow rate of 2 mL min^{-1} for subsequent determination by FAAS.

RESULTS AND DISCUSSION

Morphologic, Structural, and Thermal Characterization of PS-GO. The immobilization of oxygen abundant GO on the PS was characterized and confirmed by closer examination of SEM images, solid state ^{13}C NMR spectroscopy, FT-IR spectroscopy, and EDS spectroscopy. Figure 2A shows an SEM image of a bare PS bead with a clear and smooth surface. After GO immobilization (Figure 2B), the PS-GO shows the disordered distribution of GO sheets on to the PS beads. Furthermore, the appearance of GO wrinkles and scrolling on PS was evident from a typical TEM image (Figure 2G). The EDS results (Figure S1, Supporting Information) obtained from the SEM images (Figure 2C) of the PS-GO and their corresponding elemental mapping images (Figure 2D−F) show bright colored spots illustrating homogeneous distribution of C, O, and Pb, respectively, in the entire range. In the selected area electron diffraction (SAED) pattern (Figure 2H), the diffraction dots are absent, indicating the amorphous nature of PS-GO, which may ascribe the presence of functional groups on GO surface. The chemical shifts observed in the ^{13}C NMR spectra (Figure S6, Supporting Information) indicate the presence of an amide bond (160.9 ppm), $-CH_2-NHR$ (45.7 ppm), benzylic −C−NHR (64.4 ppm), styrenic −CH and $-CH_2$ (26−40.4 ppm), aromatic carbons (90−145.4 ppm), carboxylic carbon (175 ppm), and carbonylic carbon (206.6 ppm, 224.3 ppm). The complexation of PS-GO with Pb^{2+} was confirmed by FT-IR, FIR, and EDS analysis.

In the FT-IR spectrum of PS-GO (Figure 2I), the broad band at 3362.5 cm^{-1} corresponds to structural O−H (−COOH and −OH) stretching vibrations,[57] and the peaks at 1737 and 1025 cm^{-1} are due to C═O and C−N stretching vibrations, respectively.[58] The peaks at 1225 and 1104 cm^{-1} are associated with C−O stretching vibrations.[58] The band at 1445 and 1487 cm^{-1} may be assigned to the stretching of C═C bonds.[58] The N−H bending and wagging are indicated by the presence of peaks at 1604 cm^{-1} and at 754 and 695 cm^{-1}, respectively.[57,58] In addition, the peak at 1366 cm^{-1} can be attributed to O−H deformation.[58] The spectrum also shows the peaks at 3025 and 2920.8 cm^{-1} for sp^3 C−H and sp^2 C−H stretching vibrations, respectively.[57]

These bands become weak after Pb^{2+} sorption, and a red shift (4−6 cm^{-1}) in the bands of the C═O and N−H groups and a blue shift (5−9 cm^{-1}) in the C−O band were observed in the

FT-IR spectrum of Pb^{2+} complexed PS-GO (Figure S2, Supporting Information). In the FIR spectrum obtained after Pb^{2+} sorption (Figure S3, Supporting Information), the peak at 145 cm^{-1} indicates Pb−O vibrational frequency of the chelating active sites,[43] which confirms the complexation between Pb^{2+} and the oxygen-containing functional groups on the PS-GO. The EDS spectra also depict the complexation of Pb^{2+} with the PS-GO. The specific surface area of PS-GO estimated by BET method was found to be 12.06 m^2 g^{-1}. On the basis of the TGA/DTA curve (Figure S4, Supporting Information), the thermal stability of PS-GO was found up to 220 °C. The TGA curve shows slight weight loss after 60 °C, which is likely due to evaporation of sorbed water molecules from PS-GO, and the degradation of resin commences above 220 °C, which may attributed to the loss of CO and CO_2 from the decomposition of oxygen functional groups and carbon oxidation, respectively.[59]

Optimization of Experimental Parameters. *Effect of pH on Pb^{2+} Sorption.* Lead exists in different forms at different pH values in aqueous solution.[43,60] The extents of dissociation and metal binding ability of functional groups are also expected to be different at different pH values. Therefore, the pH of a solution plays an important role in the sorption of Pb^{2+}. As illustrated in Figure 3, the sorption capacity (Q_e; mg g^{-1}) increases significantly with increasing pH ranging from 2.0 to 7.5 due to the increase in dissociation of functional groups and the decrease in the level of competition between H^+ and Pb^{2+} for the same sorption site. Maximum uptake (227.92 mg g^{-1}) of Pb^{2+} was observed in the pH range of 7.5−8.5, because deprotonation makes the oxygen-containing GO functional groups negatively charged, which facilitates complexation with Pb^{2+} owing to the strong electrostatic interactions. Formation of hydroxide complexes ($PbOH^+$) and $Pb(OH)_2$ takes place at pH 9 and 10, and the decrease of the positive charge of hydroxide complexes decreases the electrostatic attraction, thereby decreasing Pb^{2+} sorption. At pH > 10, the predominant Pb species is $Pb(OH)^{3-}$, and the functional groups are also progressively deprotonated to form negative charge on the surface, which renders its sorption. For subsequent experiments, pH 7.5 ± 0.1 was selected as the optimum working pH to consider high sorption of Pb^{2+} and to prevent formation of Pb hydroxides.

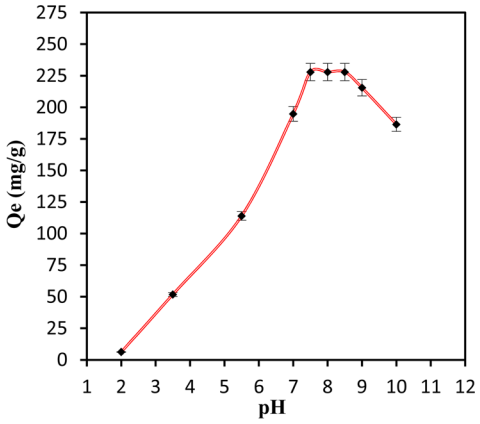

Figure 3. Effect of solution pH on the sorption of Pb on PS-GO. Experimental conditions: sample volume 50 mL; Pb, 750 μg mL^{-1}; PS-GO, 100 mg.

Effect of Stirring Time. To investigate the optimum contact time, we stirred the PS-GO with Pb^{2+} solution from 5 min to 1 h at optimized pH. Figure 4 shows that the sorption of Pb^{2+} increased remarkably at the beginning of the experiment and then reached equilibrium after 45 min. The sorption half-time ($t_{1/2}$) needed to reach 50% of the total sorption capacity is about 20 min, which reflects better accessibility of the active sites occupied on the PS-GO surface. In addition, the effect of low concentration of Pb^{2+} on the sorption rate was also studied. It was found that the sorption of Pb^{2+} reached 90% of its equilibrium just after 5 min when the loading concentration of Pb^{2+} was 50 mg L^{-1} (Figure S5, Supporting Information). It is apparent that the sorption rate is faster at a lower concentration, indicating its potential column operation for separation/preconcentration of Pb^{2+} from environmental samples.

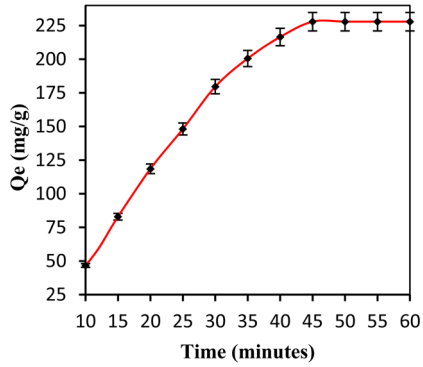

Figure 4. Effect of stirring time on the sorption of Pb on PS-GO. Experimental conditions: pH 7.5 ± 0.1; sample volume, 50 mL; Pb, 750 μg mL^{-1}; PS-GO, 100 mg.

Type of Eluting Agent and Column Reusability Test. For an ideal sorbent, the sorption capacity and the quantitative recovery of sorbed analyte are the two key parameters. For PS-GO, elution studies were accomplished by using HCl and HNO_3 with different volumes (1−10 mL) and concentrations (0.1−2.0 M). Among them, 5 mL of 2 M HNO_3 could give a maximum recovery of 95%. When 5 mL of 2 M HCl was used, almost complete desorption of Pb^{2+} (recovery >99%) was observed. The efficacy of 2 M HCl was studied at different volumes (1−10 mL). It was found that 5 mL of acid was sufficient for quantitative recovery (>99%) of the Pb^{2+} from the sorbent. Therefore, 5 mL of 2 M HCl was used for elution for further studies.

The polymer-bound GO was subjected to several loading and elution cycles by the column method. Such low concentration of the eluent acid was found to prevent any leaching of inherent toxic GO into the environment. The column bed was reused up to 50 cycles without loss of any capacity. Afterward, a gradual loss of capacity was observed, and finally, 10% loss of analyte uptake was observed in the 63rd cycle. Therefore, multiple use of the PS-GO in the separation/preconcentration of Pb^{2+} from environmental samples is feasible.

Effect of Flow Rate. To optimize the influence of column flow rate on sorption/elution, we passed a 100 mL solution containing 5 μg Pb^{2+} buffered at pH 7.5 ± 0.1 through the column in the range of 2−10 mL min^{-1}. The results showed that the quantitative retention of the analyte ion on the column was unaffected up to a flow rate of 5 mL min^{-1}, indicating a fairly fast kinetics. As we further increase the flow rate, the

retention of Pb^{2+} gradually decreases up to 55% at 8 mL min^{-1}. Hence, a 5 mL min^{-1} sorption flow rate was chosen and applied for subsequent experiments. Similarly, in the elution studies, the effect of elution flow rate was also studied using 5 mL of 2 M HCl, >99% of the retained analyte get eluted from the PS-GO at a flow rate of 2 mL min^{-1} and is considered optimum henceforth.

Effect of Foreign Ions. The ultimate aim of synthesizing this resin is to preconcentrate a trace quantity of Pb^{2+} from real samples with complex matrices where it is associated with various major coexisting ions. Usually, cations compete for the active sites of sorbent with the analyte, and anions compete for the analyte with the sorbent, which reduce the sorption of target metal ion. Moreover, the presence of alkali metals, alkaline earth metals, and certain anions exhibit interferences in the FAAS determination of analyte metal ions. An ion was considered as an interferent when it caused a variation greater than ±5% in the quantitative recovery of Pb^{2+}. To evaluate the tolerance level of PS-GO, we preconcentrated a trace quantity of Pb^{2+} following the optimized column procedure in the presence of a large amount of possibly interfering cations and anions. No significant interferences were observed in the preconcentration and FAAS determination of Pb^{2+} for all added ions (by 2−5 fold) as the percent recovery of Pb^{2+} is well above 96% (Table 1), which shows the efficiency of PS-GO in the trace determination of Pb^{2+} in the environmental and food samples.

Table 1. Effect of Foreign Ions on the Recovery of Pb^{2+}

foreign ions	added as	amount added (μg)	% recovery	RSD (N = 3)
Cl^-	NaCl	9.5×10^4	101.5	0.69
Br^-	NaBr	1.0×10^5	100.0	1.48
PO_4^{2-}	Na_2HPO_4	2.8×10^4	96.0	0.65
NO_3^-	$NaNO_3$	1.5×10^4	100.0	0.30
CO_3^{2-}	Na_2CO_3	2.8×10^3	100.0	0.97
SO_4^{2-}	Na_2SO_4	2.7×10^3	99.5	0.95
Na^+	NaCl	6.2×10^4	99.2	3.09
K^+	KCl	5.0×10^4	101.6	1.32
Ca^{2+}	$CaCl_2$	1.0×10^4	97.3	0.45
Mg^{2+}	$MgCl_2$	1.2×10^4	101.0	1.62
Zn^{2+}	$ZnCl_2$	2.5×10^2	98.4	1.15
Cd^{2+}	$CdCl_2$	3.0×10^2	98.0	1.30
Ni^{2+}	$NiNO_3$	3.0×10^2	99.6	1.40
Cu^{2+}	$CuNO_3$	2.5×10^2	96.0	1.61
Co^{2+}	$CoNO_3$	2.5×10^2	97.2	1.26
Fe^{3+}	$Fe(NO_3)_3$	3.0×10^2	99.6	2.23
Fe^{2+}	$FeSO_4$	3.0×10^2	98.2	2.50
Al^{3+}	$Al(NO_3)_3$	2.0×10^2	99.4	1.70
Ag^+	$AgNO_3$	2.5×10^2	98.3	3.20
Mn^{2+}	$MnSO_4$	3.5×10^2	97.6	2.62
Ba^{2+}	$BaCl_2$	1.5×10^4	98.0	1.89

Preconcentration Studies. To investigate the minimum concentration up to which quantitative recovery of Pb^{2+} can be achieved by applying the optimized column method, we continuously increased the volume of sample solution while keeping the total amount of loaded metal ion constant at 5 μg. Retained Pb^{2+} was quantitatively recovered up to a sample volume of 2000 mL (101%), and as we further increased the sample volume to 2200 mL, the recovery of analyte was reduced to 89.8%. Hence, the limit of preconcentration was calculated to be 2.5 μg L^{-1}, with a preconcentration factor of 400 showing the potential application of PS-GO in column preconcentration. The presence of a large number of carboxyl and hydroxyl groups introduces a strong hydrophilic character, which plays a major role in enhancing the preconcentration factor as it facilitates faster attainment of equilibrium between the resin bed and the aqueous phase.

Analytical Method Validation. The accuracy of the method was assessed by analyzing SRMs and recovery studies using optimized column procedure (Table 2). The Student's t-test values for mean concentration of Pb^{2+} in SRMs (NIES 8, 2.639; SRM 1572, 0.693) were found to be less than the critical Student's t-value of 4.303 at 95% confidence level for N = 3 (Table 2), indicating the absence of bias even in the presence of other minor and major elements. Recovery experiments were performed after spiking with two levels of known amounts of Pb^{2+} into real samples (water and food), as reported in Table 2. The mean percentage recoveries were 98.6−103.2% with relative standard deviation (RSD) <5%, thereby indicating the reliability of the present method for the determination of Pb^{2+} in real samples of various matrices without significant interference. The method had good precision, as the coefficient of variation for five replicate measurements of 5 μg Pb^{2+} in 100 mL was <5%. The calibration curve for Pb^{2+} obtained by least-squares method after preconcentrating a series of standards under optimized conditions was linear with the correlation coefficient (R^2) = 0.999 and regression equation; $A = 0.037C + 0.017$. The limit of detection and the limit of quantification, evaluated as 3 and 10 times the standard deviation of the mean blank signal (absorbance), were found to be 2.3 (−0.0001) and 7.7 μg L^{-1}, respectively, after 20 blank runs using 100 mL of aqueous solution maintained at pH of 7.5 and finally eluting the same in 5 mL before subjecting it to FAAS determination.

Application to Environmental Samples. To examine the applicability of the proposed method for practical use, we determined the Pb^{2+} concentration in various water samples (1 L) and food samples (100 mL) with a 95% confidence limit after preconcentration following the optimized column procedure and found it to be 5.13, 3.58, and 26.20 μg L^{-1} for tap water, river water, and electroplating wastewater, respectively (Table 2). Such trace concentration cannot be directly determined by FAAS because of its inherent low detection limit. Pb^{2+} content of rice and gram samples were also reported.

Comparison of PS-GO with Other SPE Methods. Direct use of GO may result in a higher sorption capacity, but its use to develop a column preconcentration/separation method is impracticable. Hence, its application is limited to batch method, which has its inherent limitations of reusability, as discussed in the Introduction. Although the numerical value of sorption capacity of PS-GO for Pb^{2+} is low compared to those of other GO matrices, it is quiet significant, considering that only a small quantity of GO is immobilized on long polymeric styrene support material used in column operation. However, only PS did not show any sorption capacity for Pb^{2+} as it does not possess any functional groups to bind metal ions. Some previous SPE works based on separation/preconcentration of Pb^{2+} are compared with our proposed method (Table 3). The comparative data indicating the superiority of our work over others mainly regards sorption capacity, detection limit, and preconcentration factor of the system apart from inherent advantages of column operation and reusability.

Table 2. Analytical Results for FAAS Determination of Pb^{2+} in Certified Reference Materials, Natural Water, and Food Samples after Column Preconcentration

samples	concentration certified ($\mu g\ g^{-1}$)[a]	concentration after SPE ($\mu g\ L^{-1}$ or $\mu g\ g^{-1}$)[a]	amount spiked (μg)	amount found in μg (RSD)	% recovery
NIES 8[b]	219.0 ± 9	201.6 ± 28.33			
SRM 1572[b]	13.3 ± 2.4	13.1 ± 1.23			
tap water[c]		5.13 ± 0.32	0	5.13 (2.55)	
			5	10.28 (2.71)	103.0
			10	15.07 (2.04)	99.4
river water[c]		3.58 ± 0.16	0	3.58 (1.80)	
			5	8.51 (2.46)	98.6
			10	13.61 (2.48)	100.3
electroplating wastewater[c]		26.20 ± 1.91	0	26.20 (2.94)	
			5	31.13 (2.91)	98.6
			10	36.52 (3.54)	103.2
rice[b]		1.06 ± 0.31	0	1.06 (1.89)	
			5	6.05 (2.30)	99.8
			10	11.32 (2.15)	102.6
gram[b]		0.42 ± 0.15	0	0.42 (4.76)	
			5	5.47 (2.21)	101.0
			10	10.48 (1.68)	100.6

[a]Mean value ±95% confidence limit. [b]$\mu g \cdot g^{-1}$. [c]$\mu g \cdot L^{-1}$; $N = 3$.

Table 3. Summary of Some Previous Solid-Phase Extraction Studies for Pb^{2+}

adsorbent	application mode	pH	capacity (mg g^{-1})	PF[a]	LOD ($\mu g\ L^{-1}$)	detection	ref
PS-GO	column	7.5	227.92	400	2.3	FAAS	this work
EDTA-GO	batch	6.8	479			AAS, ICP, and UV spectrometry	61
GO	batch	6.0	842−1850			UV spectrometry	43
magnetic MWCNT	column	9.0		390	1.0	FAAS	62
SNP loaded alumina	column	8.5	4.69	83.3	0.63	FAAS	21
graphene	column	6.0	16.6	125	0.61	FAAS	63
oxidized MWCNT	column	6.0		15.4	1.0	FAAS	64
MWCNT	column	6.0		20	8.9	FAAS	65
activated carbon	column	4−6, 10−11	2.36	80	0.92	ICP-OES	66
ion imprinted polymer	column	6.0	75.4	245	0.42	FAAS	67

[a]Preconcentration factor.

Environmental Implications. The objective to design a new solid-phase extractant is to develop an environmentally safe column preconcentration/separation method for monitoring the level of contamination by toxic environmental pollutants. As discussed in the Introduction and the Results and Discussion section, PS-GO did not release any toxic GO, even up to 50 sorption/elution cycles, and complete elution of metal ions does not involve the use of any carcinogenic organic solvents. The proposed column method was observed to show its ability to preconcentrate Pb^{2+} from a concentration as low as 2.5 $\mu g\ L^{-1}$ and its accurate determination by cheap analytical technique (FAAS) without any interference from commonly occurring cations and anions. Potential application was exhibited by the analysis of electroplating wastewater, river and tap water, and food samples for Pb^{2+} content. From the fact that sorption mechanism follows Langmuir isotherm (Table S1, Supporting Information) and PS-GO possesses reasonably high sorption capacity, its utility could further be extended for the removal of Pb^{2+} from industrial effluents. According to our literature knowledge, this is the first attempt to exploit the advantages of GO as a solid-phase extractant for detailed preconcentration studies of metal ions in column operation as evidenced from Table 3 and theIntroduction.

■ ASSOCIATED CONTENT

Ⓢ Supporting Information

PS-GO characterization reports (EDS, TGA-DTA data, and FT-IR and ^{13}C NMR spectra), and sorption isotherm studies. This material is available free of charge via the Internet at http://pubs.acs.org.

■ AUTHOR INFORMATION

Corresponding Author

*Tel.: +91 9358979659. E-mail: aminulislam.ch@amu.ac.in.

Notes

The authors declare no competing financial interest.

■ REFERENCES

(1) Hu, H. In *Harrison's Principles of Internal Medicine*; Kasper, D. L., Braunwald, E., Fauci, A. S., Hauser, S. L., Longo, D. L., Jameson, J. L., Eds.; McGraw-Hill: New York, 2005; Chapter 376, pp 2577−2580.

(2) Neala, A. P.; Tomas, R. G. Mechanisms of Lead and Manganese Neurotoxicity. *Toxicol. Res.* **2013**, *2*, 99−114.

(3) Elci, L.; Arslan, Z.; Tyson, J. Determination of Lead in Wine and Rum Samples by Flow Injection-Hydride Generation-Atomic Absorption Spectrometry. *J. Hazard. Mater.* **2009**, *162*, 880−885.

(4) Karadjova, I.; Lampugnani, L.; Dulivo, A.; Onor, M.; Tsalev, D. Determination of Lead in Wine by Hydride Generation Atomic

Fluorescence Spectrometry in the Presence of Hexacyanoferrate(III). *Anal. Bioanal. Chem.* **2007**, *388*, 801−807.
(5) *Fact Sheet for Medium-Sized Water Systems: Lead and Copper Rule Minor Revisions*; EPA 816-F-00-008; United States Environmental Protection Agency (USEPA) Office of Water: Washington, DC, 2001.
(6) *Guidelines for Drinking-Water Quality Health Criteria and other Supporting Information*; World Health Organization (WHO): Geneva, Switzerland, 1996.
(7) Dong, Y.; Tian, W.; Ren, S.; Dai, R.; Chi, Y.; Chen, G. Graphene Quantum Dots/L-Cysteine Coreactant Electrochemiluminescence System and Its Application in Sensing Lead(II) Ions. *ACS Appl. Mater. Interfaces* **2014**, *6*, 1646−1651.
(8) Chai, F.; Wang, C.; Wang, T.; Li, L.; Su, Z. Colorimetric Detection of Pb^{2+} Using Glutathione Functionalized Gold Nanoparticles. *ACS Appl. Mater. Interfaces* **2010**, *2*, 1466−1470.
(9) Xiang, Y.; Tong, A.; Lu, Y. Abasic Site-Containing DNAzyme and Aptamer for Label-Free Fluorescent Detection of Pb^{2+} and Adenosine with High Sensitivity, Selectivity, and Tunable Dynamic Range. *J. Am. Chem. Soc.* **2009**, *131*, 15352−15357.
(10) Li, C.; Wei, L.; Liu, X.; Lei, L.; Li, G. Ultrasensitive Detection of Lead Ion Based on Target Induced Assembly of DNAzyme Modified Gold Nanoparticle and Graphene Oxide. *Anal. Chim. Acta* **2014**, *831*, 60−64.
(11) Khajeh, M.; Laurent, S.; Dastafkan, K. Nanoadsorbents: Classification, Preparation, and Applications (with Emphasis on Aqueous Media). *Chem. Rev.* **2013**, *113*, 7728−7768.
(12) Das, D.; Gupta, U.; Das, A. K. Recent Developments in Solid Phase Extraction in Elemental Speciation of Environmental Samples with Special Reference to Aqueous Solutions. *TrAC, Trends Anal. Chem.* **2012**, *38*, 163−171.
(13) Pyrzynska, K. Carbon Nanostructures for Separation, Preconcentration, and Speciation of Metal Ions. *Trends Anal. Chem.* **2010**, *29*, 718−727.
(14) Chen, Y.; Pan, B.; Li, H.; Zhang, W.; Lv, L.; Wu, J. Selective Removal of Cu(II) Ions by Using Cation-Exchange Resin-Supported Polyethyleneimine (PEI) Nanoclusters. *Environ. Sci. Technol.* **2010**, *44*, 3508−3513.
(15) Karadas, C.; Kara, D.; Fisher, A. Determination of Rare Earth Elements in Seawater by Inductively Coupled Plasma Mass Spectrometry with Off-Line Column Preconcentration Using 2,6-Diacetylpyridine Functionalized Amberlite XAD-4. *Anal. Chim. Acta* **2011**, *689*, 184−189.
(16) Islam, A.; Ahmad, A.; Laskar, M. A. A Newly Developed Salicylanilide Functionalized Amberlite XAD-16 Chelating Resin for Use in Preconcentration and Determination of Trace Metal Ions from Environmental and Biological Samples. *Anal. Methods* **2011**, *3*, 2041−2048.
(17) Islam, A.; Ahmad, H.; Zaidi, N.; Yadav, S. Selective Separation of Aluminum from Biological and Environmental Samples Using Glyoxal-bis(2-hydroxyanil) Functionalized Amberlite XAD-16 Resin: Kinetics and Equilibrium Studies. *Ind. Eng. Chem. Res.* **2013**, *52*, 5213−5220.
(18) Islam, A.; Laskar, M. A.; Ahmad, A. Characterization and Application of 1-(2-Pyridylazo)-2-naphthol Functionalized Amberlite XAD-4 for Preconcentration of Trace Metal Ions in Real Matrices. *J. Chem. Eng. Data* **2010**, *55*, 5553−5561.
(19) Islam, A.; Ahmad, A.; Laskar, M. A. Preparation, Characterization of a Novel Chelating Resin Functionalized with o-Hdroxybenzamide and Its Application for Preconcentration of Trace Metal Ions. *Clean: Soil, Air, Water* **2012**, *40*, 54−65.
(20) Islam, A.; Ahmad, A.; Laskar, M. A. Characterization of a Chelating Resin Functionalized via Azo Spacer and Its Analytical Applicability for the Determination of Trace Metal Ions in Real Matrices. *J. Appl. Polym. Sci.* **2012**, *123*, 3448−3458.
(21) Ghanemi, K.; Nikpour, Y.; Omidvar, O.; Maryamabadi, A. Sulfur-Nanoparticle-Based Method for Separation and Preconcentration of Some Heavy Metals in Marine Samples Prior to Flame Atomic Absorption Spectrometry Determination. *Talanta* **2011**, *85*, 763−769.
(22) Baytaka, S.; Zereen, B.; Arslan, Z. Preconcentration of Trace Elements from Water Samples on a Minicolumn of Yeast (Yamadazyma Spartinae) Immobilized TiO_2 Nanoparticles for Determination by ICP-AES. *Talanta* **2011**, *84*, 319−323.
(23) Tian, X.; Zhou, S.; Zhang, Z.; He, X.; Yu, M.; Lin, D. Metal Impurities Dominate the Sorption of a Commercially Available Carbon Nanotube for Pb(II) from Water. *Environ. Sci. Technol.* **2010**, *44*, 8144−8149.
(24) Zhang, X.; Kah, M.; Jonker, M. T. O.; Hofmann, T. Dispersion State and Humic Acids Concentration-Dependent Sorption of Pyrene to Carbon Nanotubes. *Environ. Sci. Technol.* **2012**, *46*, 7166−7173.
(25) Vallent, R. M.; Szabo, Z.; Bachmann, A.; Bakry, R.; Najam-ul-Haq, M.; Rainer, M.; Heigl, N.; Huck, C. W.; Bonn, G. K. Development and Application of C60-Fullerene Bound Silica for Solid-Phase Extraction of Biomolecules. *Anal. Chem.* **2007**, *79*, 8144−8153.
(26) Zhua, S.; Niu, W.; Li, H.; Han, S.; Xu, G. Single-Walled Carbon Nanohorn as New Solid-Phase Extraction Adsorbent for Determination of 4-Nitrophenol in Water Sample. *Talanta* **2009**, *79*, 1441−1445.
(27) He, Q.; Hu, Z.; Jiang, Y.; Chang, X.; Tu, Z.; Zhang, L. Preconcentration of Cu(II), Fe(III), and Pb(II) with 2-((2-Aminoethylamino)methyl)phenol-Functionalized Activated Carbon Followed by ICP-OES Determination. *J. Hazard. Mater.* **2010**, *175*, 710−714.
(28) Sulaymon, A. H.; Ahmed, K. W. Competitive Adsorption of Furfural and Phenolic Compounds onto Activated Carbon in Fixed Bed Column. *Environ. Sci. Technol.* **2008**, *42*, 392−397.
(29) Jimenez-Soto, J. M.; Cardenas, S.; Valcarcel, M. Evaluation of Carbon Nanocones/Disks as Sorbent Material for Solid-Phase Extraction. *J. Chromatogr. A* **2009**, *1216*, 5626−5633.
(30) Pumera, M.; Miyahara, Y. What Amount of Metallic Impurities in Carbon Nanotubes is Small Enough Not to Dominate their Redox Properties? *Nanoscale* **2009**, *1*, 260−265.
(31) Banks, C. E.; Crossley, E.; Salter, C.; Wilkins, S. J.; Compton, R. G. Carbon Nanotubes Contain Metal Impurities Which are Responsible for the "Electrocatalysis" Seen at Some Nanotube-Modified Electrodes. *Angew. Chem., Int. Ed.* **2006**, *45*, 2533−2537.
(32) Geim, A. K.; Novoselov, K. S. The Rise of Graphene. *Nat. Mater.* **2007**, *6*, 183−191.
(33) Bae, S. K.; Kim, H.; Lee, Y. B.; Xu, X. F.; Park, J. S.; Zheng, Y.; Balakrishnan, J.; Lei, T.; Kim, H. R.; Song, Y. I.; Kim, Y.; Kim, K. S.; Ozyilmaz, B.; Ahn, J.; Hong, B. H.; Iijima, S. Roll-to-Roll Production of 30 Inch Graphene Films for Transparent Electrodes. *Nat. Nanotechnol.* **2010**, *5*, 574−578.
(34) Geim, A. K. Graphene: Status and Prospects. *Science* **2009**, *324*, 1530−1534.
(35) Zhao, G. X.; Jiang, L.; He, Y. D.; Li, J. X.; Dong, H. K.; Wang, X. K.; Hu, W. P. Sulfonated Graphene for Persistent Aromatic Pollutant Management. *Adv. Mater.* **2011**, *23*, 3959−3963.
(36) Cai, B.; Lv, X.; Gan, S.; Zhou, M.; Ma, W.; Wu, T.; Li, F.; Han, D.; Niu, L. Advanced Visible-Light-Driven Photocatalyst Upon the Incorporation of Sulfonated Graphene. *Nanoscale* **2013**, *5*, 1910−1916.
(37) Lee, T.; Yun, T.; Park, B.; Sharma, B.; Song, H.; Kim, B. Hybrid Multilayer Thin Film Supercapacitor of Graphene Nanosheets with Polyaniline: Importance of Establishing Intimate Electronic Contact through Nanoscale Blending. *J. Mater. Chem.* **2012**, *22*, 21092−21099.
(38) Chang, H.; Tang, L.; Wang, Y.; Jiang, J.; Li, J. Graphene Fluorescence Resonance Energy Transfer Aptasensor for the Thrombin Detection. *Anal. Chem.* **2010**, *82*, 2341−2346.
(39) Zhang, K.; Zhang, L. L.; Zhao, X. S.; Wu, J. Graphene/Polyaniline Nanofiber Composites as Supercapacitor Electrodes. *Chem. Mater.* **2010**, *22*, 1392−1401.
(40) Sun, Y.; Shao, D.; Chen, C.; Yang, S.; Wang, X. Highly Efficient Enrichment of Radionuclides on Graphene Oxide-Supported Polyaniline. *Environ. Sci. Technol.* **2013**, *47*, 9904−9910.
(41) Yang, S. T.; Chang, Y. L.; Wang, H. F.; Liu, G. B.; Chen, S.; Wang, Y. W.; Liu, Y. F.; Cao, A. N. Folding/Aggregation of Graphene Oxide and Its Application in Cu^{2+} Removal. *J. Colloid Interface Sci.* **2010**, *351*, 122−127.

(42) Zhao, G. X.; Li, J. X.; Ren, X. M.; Chen, C. L.; Wang, X. K. Few-Layered Graphene Oxide Nanosheets as Superior Sorbents for Heavy Metal Ion Pollution Management. *Environ. Sci. Technol.* **2011**, *45*, 10454−10462.
(43) Zhao, G.; Ren, X.; Gao, X.; Tan, X.; Li, J.; Chen, C.; Huang, Y.; Wang, X. Removal of Pb(II) Ions from Aqueous Solutions on Few-Layered Graphene Oxide Nanosheets. *Dalton Trans.* **2011**, *40*, 10945−10952.
(44) Sitko, R.; Turek, E.; Zawisza, B.; Malicka, E.; Talik, E.; Heimann, J.; Gagor, A.; Feista, B.; Wrzalik, R. Adsorption of Divalent Metal Ions from Aqueous Solutions Using Graphene Oxide. *Dalton Trans.* **2013**, *42*, 5682−5689.
(45) Chandra, V.; Park, J.; Chun, Y.; Lee, J. W.; Hwang, I.; Kim, K. S. Water-Dispersible Magnetite-Reduced Graphene Oxide Composites for Arsenic Removal. *ACS Nano* **2010**, *4*, 3979−3986.
(46) Sun, Y.; Wang, Q.; Chen, C.; Tan, X.; Wang, X. Interaction Between Eu(III) and Graphene Oxide Nano Sheets Investigated by Batch and Extended X-ray Absorption Fine Structure Spectroscopy and by Modeling Techniques. *Environ. Sci. Technol.* **2012**, *46*, 6020−6027.
(47) Li, J.; Zhang, S.; Chen, C.; Zhao, G.; Yang, X.; Li, J.; Wang, X. Removal of Cu(II) and Fulvic Acid by Graphene Oxide Nano Sheets Decorated with Fe_3O_4 Nanoparticles. *ACS Appl. Mater. Interfaces* **2012**, *4*, 4991−5000.
(48) Deng, D.; Jiang, X.; Yang, L.; Hou, X.; Zheng, C. Organic Solvent-Free Cloud Point Extraction-like Methodology Using Aggregation of Graphene Oxide. *Anal. Chem.* **2014**, *86*, 758−765.
(49) Lerf, A.; He, H.; Forster, M.; Klinowski, J. Structure of Graphite Oxide Revisited[II]. *J. Phys. Chem. B* **1998**, *102*, 4477−4482.
(50) Liu, Q.; Shi, J.; Zeng, L.; Wang, T.; Cai, Y.; Jiang, G. Evaluation of Graphene as an Advantageous Adsorbent for Solid-Phase Extraction with Chlorophenols as Model Analytes. *J. Chromatogr. A* **2011**, *1218*, 197−204.
(51) Duch, M. C.; Budinger, G. R. S.; Liang, Y. T.; Soberanes, S.; Urich, D.; Chiarella, S. E.; Campochiaro, L. A.; Gonzalez, A.; Chandel, N. S.; Hersam, M. C.; Mutlu, G. M. Minimizing Oxidation and Stable Nanoscale Dispersion Improves the Biocompatibility of Graphene in the Lung. *Nano Lett.* **2011**, *11*, 5201−5207.
(52) Chang, Y. L.; Yang, S. T.; Liu, J. H.; Dong, E.; Wang, Y. W.; Cao, A. N.; Liu, Y. F.; Wang, H. F. In Vitro Toxicity Evaluation of Graphene Oxide on A549 Cells. *Toxicol. Lett.* **2011**, *200*, 201−210.
(53) Hummers, W. S.; Offeman, R. E. Preparation of Graphitic Oxide. *J. Am. Chem. Soc.* **1958**, *80*, 1339−1339.
(54) Liu, Q.; Shi, J.; Sun, J.; Wang, T.; Zeng, L.; Jiang, G. Graphene and Graphene Oxide Sheets Supported on Silica as Versatile and High-Performance Adsorbents for Solid-Phase Extraction. *Angew. Chem., Int. Ed.* **2011**, *50*, 5913−5917.
(55) Islam, A.; Laskar, M. A.; Ahmad, A. Characterization of a Novel Chelating Resin of Enhanced Hydrophilicity and Its Analytical Utility for Preconcentration of Trace Metal Ions. *Talanta* **2010**, *81*, 1772−1780.
(56) Islam, A.; Laskar, M. A.; Ahmad, A. Preconcentration of Metal Ions through Chelation on a Synthesized Resin Containing O, O Donor Atoms for Quantitative Analysis of Environmental and Biological Samples. *Environ. Monit. Assess.* **2013**, *185*, 2691−2704.
(57) Drago, R. S. *Physical Methods in Inorganic Chemistry*; Reinhold Publishing Corp.: New York, 1965.
(58) Socrates, G. *Infrared Characteristics Group Frequencies*, 3rd ed; Wiley InterScience: New York, 1980.
(59) Wang, G. X.; Yang, J.; Park, J.; Gou, X. L.; Wang, B.; Liu, H.; Yao, J. Facile Synthesis and Characterization of Graphene Nanosheets. *J. Phys. Chem. C* **2008**, *112*, 8192−8195.
(60) Weng, C. H. Modeling Pb(II) Adsorption onto Sandy Loam Soil. *J. Colloid Interface Sci.* **2004**, *272*, 262−270.
(61) Madadrang, C. J.; Kim, H. Y.; Gao, G.; Wang, N.; Zhu, J.; Feng, H.; Gorring, M.; Kasner, M. L.; Hou, S. Adsorption Behavior of EDTA-Graphene Oxide for Pb (II) Removal. *ACS Appl. Mater. Interfaces* **2012**, *4*, 1186−1193.
(62) Tarigh, G. D.; Shemirani, F. Magnetic Multi-Wall Carbon Nanotube Nano Composite as an Adsorbent for Preconcentration and Determination of Lead (II) and Manganese (II) in Various Matrices. *Talanta* **2013**, *15*, 744−750.
(63) Wang, Y.; Gao, S.; Zang, X.; Li, J.; Ma, J. Graphene-Based Solid-Phase Extraction Combined with Flame Atomic Absorption Spectrometry for a Sensitive Determination of Trace Amounts of Lead in Environmental Water and Vegetable Samples. *Anal. Chim. Acta* **2012**, *716*, 112−118.
(64) Zhao, X.; Song, N.; Jia, Q.; Zhou, W. Determination of Cu, Zn, Mn, and Pb by Microcolumn Packed with Multiwalled Carbon Nanotubes On-Line Coupled with Flame Atomic Absorption Spectrometry. *Microchim. Acta* **2009**, *166*, 329−335.
(65) Soylak, M.; Yilmaz, E.; Ghaedi, M.; Montazerozohori, M. Solid Phase Extraction on Multiwalled Carbon Nanotubes and Flame Atomic Absorption Spectrometry Combination for Determination of Some Metal Ions in Environmental and Food Samples. *Toxicol. Environ. Chem.* **2011**, *93*, 873−885.
(66) Feist, B.; Mikula, M. Preconcentration of Heavy Metals on Activated Carbon and Their Determination in Fruits by Inductively Coupled Plasma Optical Emission Spectrometry. *Food Chem.* **2014**, *147*, 302−306.
(67) Behbahani, M.; Bagheri, A.; Taghizadeh, M.; Salarian, M.; Sadeghi, O.; Adlnasab, L.; Jalali, K. Synthesis and Characterisation of Nano Structure Lead(II) Ion-Imprinted Polymer as a New Sorbent for Selective Extraction and Preconcentration of Ultra Trace Amounts of Lead Ions from Vegetables, Rice, and Fish Samples. *Food Chem.* **2013**, *138*, 2050−2056.